

Therapeutic Potential of Surface Functionalized Mn₃O₄ Nanoparticles Against Chronic Liver Diseases in Murine Model

Aniruddha Adhikari¹, Nabarun Polley¹, Soumendra Darbar², and Samir Kumar Pal^{1,*}

¹Department of Chemical, Biological and Macromolecular Sciences, S. N. Bose National Centre for Basic Sciences, Block JD, Sector III, Salt Lake, Kolkata 700106, India

²Research and Development Division, Dey's Medical Stores (Mfg.) Ltd., 62, Bondel Road, Ballygunge, Kolkata 700019, India

ABSTRACT

Currently there is a great deal of interest on health benefits of inorganic nanoparticles. Although they have been successfully introduced against several diseases, their direct use in treatment of chronic diseases are sparse in literature. Chronic liver diseases are the fifth most common cause of death, affecting around 400 million people per year worldwide and have no effective medication. The aim of this study was to evaluate potential hepatoprotective activity of orally administered citrate functionalized Mn₃O₄ nanoparticles (C-Mn₃O₄ NPs) against CCl₄ induced hepatotoxicity. Our results show that oral treatment of C-Mn₃O₄ NPs can effectively reduce severe chronic liver damage even fibrosis in CCl₄-induced mice model. Further investigations revealed that C-Mn₃O₄ NPs show increased antioxidant activity upon acid treatment (both *in vitro* and *in vivo* i.e., stomach), which is in turn responsible for its hepatoprotective nature. Assessment of various liver function parameters along with histopathology and immunohistochemistry were performed to evaluate pathophysiological condition of the liver. To unravel the mechanisms involved in attenuation of liver injury by NPs, various antioxidant parameters (like superoxide dismutase, catalase, glutathione peroxidase, reduced glutathione etc.) were also examined. An in depth study of the effect of C-Mn₃O₄ NPs on mitochondria, the cellular mediator of oxidative stress further revealed the molecular mechanism behind its therapeutic efficacy. To best of our knowledge, this is the first study that demonstrates direct oral treatment of an inorganic NPs (i.e., C-Mn₃O₄ NPs) without any delivery system can efficiently reduce chronic hepatotoxicity and liver fibrosis through its antioxidant activity.

KEYWORDS: Nanomedicine, Hepatic Fibrosis, Antioxidant, Mice Model, Hepatotoxicity.

1. INTRODUCTION

Hepatic fibrosis is the final, common pathological outcome of chronic liver injury from a number of causes including alcohol, toxin, and persistent viral and helminthic infections.¹ Fibrosis, or scarring, is defined by the accumulation of fibrous connective tissue (components of the extracellular matrix (ECM) such as collagen and fibronectin) in and around inflamed or damaged tissue. If highly progressive, the fibrotic process eventually leads to end organ failure, hepatic carcinoma and, ultimately, death.² According to the Office for National statistics in the United Kingdom, liver disease is the fifth most common cause of death after heart disease, stroke, chest disease and cancer.³ Recent World Health Organization fact

sheets (updated in June 2014) show that out of more than 400 million detected cases of potentially life-threatening liver infection, more than 1.3 million people die every year due to acute or chronic consequences of advanced liver damage.⁴ On the other hand, there is hardly any drug available for effective long term treatment of chronic liver diseases with no or minimal side effects.⁵⁻⁸ Therefore, it is necessary and of considerable interest to develop new medicines for treatment of chronic liver diseases.

Currently, there is a great deal of interest in the health benefits of inorganic nanoparticles. But one of the major problems in application of nanomedicine against chronic diseases is its route of administration.⁹ For long term therapy, oral administration of drugs are mostly preferred due to their convenience and compliance. But unfortunately, NPs are not sufficiently effective because of their non-specific distribution to the entire body, metabolism in the GI tract, low retention in the lesion area and undesired adverse effects.¹⁰

*Author to whom correspondence should be addressed.

Email: skpal@bose.res.in

Received: 3rd October, 2016

Accepted: 5th December, 2016

In the present study, we have demonstrated the potential of orally administered C-Mn₃O₄ NPs in effective treatment of severe liver damage in CCl₄-intoxicated mice model. To the best of our knowledge, this is the first study that demonstrates direct oral treatment of an inorganic NP (i.e., C-Mn₃O₄ NP) without any delivery system can efficiently reduce chronic hepatotoxicity and liver fibrosis through its pH dependent antioxidant activity.

2. EXPERIMENTAL SECTION

2.1. Materials

Ethanol amine, hydrochloric acid (HCl), sulfuric acid (H₂SO₄), hydrogen peroxide (H₂O₂, 2[×]7[×] dichlorofluorescein diacetate (DCFH-DA), and glycerol were obtained from Merck (NJ, USA). Other chemicals were purchased from Sigma-Aldrich (MO, USA). As aqueous solvent Millipore water was used whenever required. All the chemicals used for this study were of analytical grade and used without further purification.

2.2. Synthesis of C-Mn₃O₄ NPs

For template free synthesis of bulk Mn₃O₄ NPs at normal temperature and pressure we followed a bottom up approach reported earlier.^{11 12} Surface functionalization with citrate, was done in the following way. Firstly, as prepared Mn₃O₄ NPs were added to 0.5 M aqueous ligand (citrate) solution of pH 7.0 (~20 mg Mn₃O₄ NPs/ml ligand solution) and extensively mixed for 12 hrs in a cyclomixer. A syringe filter of 0.22 μm diameter was used to eliminate the nonfunctionalized bigger-sized NPs.

2.3. Preparation of Acid Treated NPs

To mimic the acidic condition of stomach, C-Mn₃O₄ NPs were kept in 0.1 M sodium citrate buffer (pH 3.8) for 30 mins. Then they were transferred to 0.01 M phosphate buffered saline (PBS) (pH 7.4) for further studies (1:10 w/v).

2.4. Characterization Techniques

An FEI TecnaiTF-20 field emission HRTEM operating at 200 kV was used for obtaining transmission electron microscopy (TEM) and High-resolution TEM (HRTEM) images. Samples were prepared by dropwise addition of NP solution (both normal and acid treated) on 300-mesh carbon-coated copper grid and dried overnight at room temperature. Absorbance spectra were recorded in Shimadzu Model UV-2600 spectrophotometer. All fluorescence studies were performed using Jobin Yvon Model Fluoromax-3 spectrofluorimeter.

2.5. ROS Generation and Free Radical Scavenging Activity of C-Mn₃O₄ NPs

In vitro ROS generation ability of the NPs and acid treated NPs were evaluated using DCFH following a reported

method without any modification.¹³ Free radical scavenging activity of NPs and acid treated NPs were determined using the DPPH method reported earlier.¹⁴ The DPPH· radical scavenging capacity was calculated using the following equation:

$$\text{DPPH}^{\cdot} \text{ scavenging capacity (\%)} = \left(1 - \frac{\text{Abs}_{\text{SAMPLE}}}{\text{Abs}_{\text{CONTROL}}} \right) \times 100 \quad (1)$$

2.6. Animals

Healthy Swiss albino mice of either sex (5–7-weeks old, weighing 27 ± 4 gm) were used in this study. Animals were housed in standard, clean polypropylene cages and maintained in controlled laboratory environment (temperature 22 ± 3 °C; relative humidity 45–60%; 12 hrs light/dark cycle). Water and standard laboratory pellet diet for mice (Hindustan Lever, Kolkata) were available *ad libitum* throughout the experimental period. All mice were allowed to acclimatize for one week prior to experimentation. All animals received human care according to the criteria outlined by the Committee for the Purpose of Control and Supervision of Experiments on Animals (CPCSEA), New Delhi, India and the study was approved by the Institutional Animal Ethics Committee (Approval number-Dey's/IAEC/PHA/14/15, dated 31.01.2015).

2.7. Acute Toxicity Study

Single-dose oral toxicity study was conducted to determine the possible acute toxicity of C-Mn₃O₄ NPs following the general principles of the OECD guideline 423 with some adjustments.¹⁵ Twelve female mice were divided in four groups: one control group (received 0.2 ml MilliQ water) and three experimental groups (received either 500, 2000 or 5000 mg/kg body weight (BW) of NPs). All the animals were kept in fasting condition overnight prior to feeding. Behavior, mortality and body weight were monitored daily for a period of 14 days.

2.8. *In Vivo* Distribution of NPs

The manganese contents in the liver (24 hrs after treatment) and blood (2 hrs after treatment) were estimated using inductively coupled plasma atomic emission spectroscopy (ICP-AES; ARCOS, Simultaneous ICP Spectrometer, SPECTRO Analytical Instruments GmbH, Germany) at SAIF, IIT Bombay, India. The samples were prepared using open acid digestion method. In brief, dried tissue were dissolved in HNO₃ (15 ml), H₂SO₄ (10 ml), and H₂O₂ (5 ml), heated at 120 °C until only a residue remained and then diluted with deionized water to 10 mL.

2.9. Treatment Protocol

The animals were randomized into eight groups (*n* = 10 in each group). The division of groups and treatment protocol is described below.

Group I: Sham Control (2.4 ml/kg BW Olive Oil/day for 8 weeks)

Group II: CCl₄ Control (CCl₄ + Olive Oil (1:4 solution) 3 ml/kg BW/alternative day for 8 weeks)

Group III: NP Control (C-Mn₃O₄ NPs 1.5 ml/kg BW/day for 2 weeks)

Group IV: NP Treated (CCl₄ + Olive Oil (1:4 solution) 3 ml/kg BW/alternative day for 8 weeks then C-Mn₃O₄ NPs 1.5 ml/kg BW/day for 2 weeks)

Group V: Citrate Control (CCl₄ + Olive Oil (1:4 solution) 3 ml/kg BW/alternative day for 8 weeks then Citrate 0.75 ml/kg BW/day for 2 weeks)

Group VI: Standard Drug Treated (CCl₄ + Olive Oil (1:4 solution) 3 ml/kg BW/alternative day for 8 weeks then Silymarin 1.5 ml/kg BW/day for 2 weeks).

All treatments were done via oral administration. At the end of the experiment, the animals were kept in fasting condition overnight and sacrificed by cervical dislocation.

2.10. Histopathological Examination

After collection of blood, liver was excised, washed with ice-cold phosphate buffer and dried with tissue paper. It was weighed and fixed in neutral formalin solution (10%), dehydrated in graduated ethanol (50–100%), cleared in xylene and embedded in paraffin. 4–5 μm thick sections were cut, deparaffinized, hydrated and stained with hematoxylin and eosin (H/E).

2.11. Immunohistochemistry (IHC)

Paraffin-fixed liver tissue slices were sectioned, deparaffinized, rehydrated, and immersed in 3% H₂O₂ for 10 min to block endogenous peroxidase activity. Antigen retrieval was performed in citrate buffer (pH 6.0) in a microwave oven for 15 min. Bovine serum albumin (BSA) (5%) was used to block non-specific protein binding. The sections were incubated with α-SMA primary antibody overnight at 4 °C. The sections were subsequently washed with PBS and incubated with horseradish peroxidase (HRP)-conjugated goat anti-mouse IgG secondary antibodies, followed by incubation for 5–10 min with 3,3'-diaminobenzidine tetrachloride. Stained slides were analyzed using high-power field images captured under microscope (magnification × 400) (Olympus BX51). Computer-assisted semi-quantitative analysis was used to evaluate the α-SMA positive areas using ImageJ software following reported literature.¹⁶ The data for α-SMA staining was expressed as the mean percentage of the positively stained area over the total tissue section area.

2.12. Scoring of Fibrosis

Scoring of fibrosis was done by an independent pathologist unaware of the experiment using random microscopic field images of H/E, MT and IHC stained liver sections. For the scoring of hepatic necrosis we used METAVIR system

as well as Ishak Modified Hepatic Activity Index (HAI). Fibrosis score was calculated following both original and modified Ishak Staging.

2.13. Serum Isolation

For biochemical studies, blood samples were collected in sterile tubes (nonheparinized) from retro-orbital plexus just before sacrifice and allowed to clot for 45 min. Serum was separated by centrifugation at 3000 rpm for 15 min.

2.14. Measurement of Liver Function Enzymes

Sterile, hemolysis-free serum samples kept at –20 °C were used for determination of the biochemical parameters. The activities of alanine aminotransferase (ALT), aspartate aminotransferase (AST), γ-glutamyltransferase (GGT), alkaline phosphatase (ALP), total bilirubin, direct bilirubin and total protein in plasma were determined using commercially available test kits (Autospan Liquid Gold, Span Diagnostics Ltd., India) following the protocols described by the corresponding manufacturers.

2.15. Liver Homogenate Preparation

Samples of liver tissue were collected, homogenized in cold 0.1 mM phosphate buffer (pH 7.4), and centrifuged at 10,000 rpm at 4 °C for 15 mins. The supernatants were collected to determine the activity of SOD, CAT, GSH-Px and GSH as well as the content of MDA.

2.16. Assessment of Lipid Peroxidation and Hepatic Antioxidant Status

The supernatants were used to determine the activity of SOD, CAT, GSH-Px and GSH as well as the content of MDA. Degree of lipid peroxidation was determined in terms of thiobarbituric acid reactive substances (TBARS) formation using a reported procedure.¹⁷ SOD and CAT activities were estimated following methods described by Kakkar et al.¹⁸ and Britton and Mehley¹⁹ respectively. Hepatic GSH level was determined by the method of Ellman with slight modification.²⁰

2.17. Mitochondria Isolation

Mitochondria were isolated from mouse livers according to the method of Graham,²¹ with some slight modifications. In brief, livers were excised and homogenized in liver homogenization medium containing 225 mM D-mannitol, 75 mM sucrose, 0.05 mM EDTA, 10 mM KCl, 10 mM HEPES (pH 7.4). The homogenates were centrifuged at 600 × g for 15 min and resulting supernatant were centrifuged at 8500 × g for 10 min. The pellet were washed thrice and resuspended in same buffer. All procedures were done at 4 °C. Protein concentration were determined using commercially available kit (Autospan Liquid Gold, Span Diagnostics Ltd., India) following the protocol described by the manufacturer.

2.18. Cytochrome C Oxidase (COX) Activity

COX activity was measured spectrophotometrically using isolated mitochondria.²² Briefly, reduced cytochrome c was prepared by mixing cytochrome c and ascorbic acid in potassium phosphate buffer. COX activity was taken as the rate of ferrocytochrome c oxidation to ferricytochrome c, detected as the decrease in absorbance at 550 nm.

2.19. Measurement of Mitochondrial Membrane Permeability Transition (MPT)

Opening of the pore causes mitochondrial swelling, which results in reduction of absorbance at 540 nm. Mitochondrial permeability transition (swelling assay) was monitored as changes at 540 nm at 10 sec intervals over 10 min time with 250 μ g mitochondrial protein in the swelling buffer, which contains 120 mM KCl (pH 7.4) and 5 mM KH₂PO₄.

2.20. Statistical Analysis

All quantitative data are expressed as mean \pm standard deviation (SD) unless otherwise stated. One-way analysis of variance (ANOVA) followed by Tukey's multiple comparison test was executed for comparison of different parameters between the groups using a computer program GraphPad Prism (version 5.00 for Windows), GraphPad Software, California, USA. $p < 0.05$ was considered significant.

3. RESULTS AND DISCUSSION

The present study was performed with the aim of exploring the potential therapeutic effect of C-Mn₃O₄ NPs as

orally administered drug against chronic liver diseases. The C-Mn₃O₄ NPs used in this study were approximately spherical (Fig. 1(a)), with mean particle size: 6.19 ± 0.05 nm (Fig. 1(c)). HRTEM image of single NP (Fig. 1(b)) shows interfringe distance to be 0.312 nm (corresponding to the (112) planes of the Mn₃O₄ tetragonal crystal lattice) confirming its crystallinity. The absorbance spectra of the NPs and the capping ligand citrate are illustrated in Figure 1(d). A magnified view of the absorption spectrum of the NPs (400–800 nm) is represented in the inset of Figure 1(d). The observed absorbance peak at around 290 nm signifies high-energy ligand to-metal charge transfer (LMCT) transition involving citrate–Mn⁴⁺ interaction. 429, 526, 746 nm absorbance maxima are corresponding to the Jahn–Teller (J–T) distorted d–d transitions centered over Mn³⁺ ions. The NPs are also found to be fluorescent under various excitation wavelengths as reported earlier (Fig. 1(e)).^{12–23}

As all orally applied drugs need to pass through highly acidic stomach before entering hepatic circulation, it is of considerable interest to study the effect of acidic environment (of stomach) on activity and physicochemical properties of NPs. The property of C-Mn₃O₄ NPs to degrade bilirubin in dark²⁴ was monitored as a method for comparing the activities of neutral and acid treated NPs'. Figure 2(a) clearly shows an increase in bilirubin degradation activity of NPs upon acid treatment. The increased catalytic activity caused by acid treatment is in agreement with the fact that, at higher pH, Mn³⁺ in the NPs surface is stable due to comproportionation of Mn²⁺ and Mn⁴⁺ and does not tend to react with bilirubin.²⁴ In acidic pH, Mn³⁺ ions are unstable and tend to disproportionate

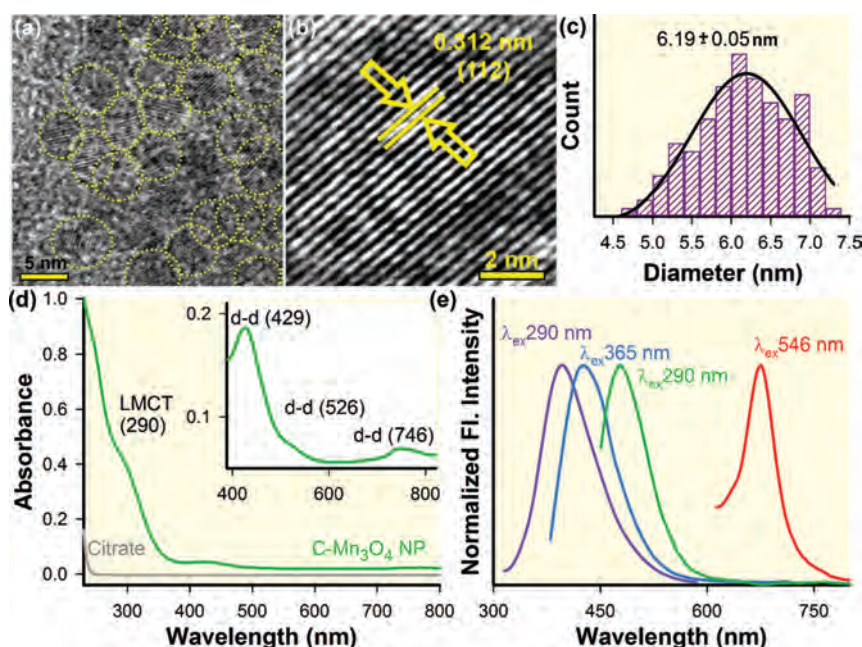


Fig. 1. Characterization of C-Mn₃O₄ NPs. (a) TEM image of the NPs. (b) HRTEM image of the NPs showing interfringe distance. (c) Size distribution of the NPs. (d & d inset) Absorbance spectrum of the NPs in aqueous solution. (e) Fluorescence emission spectra of the same.

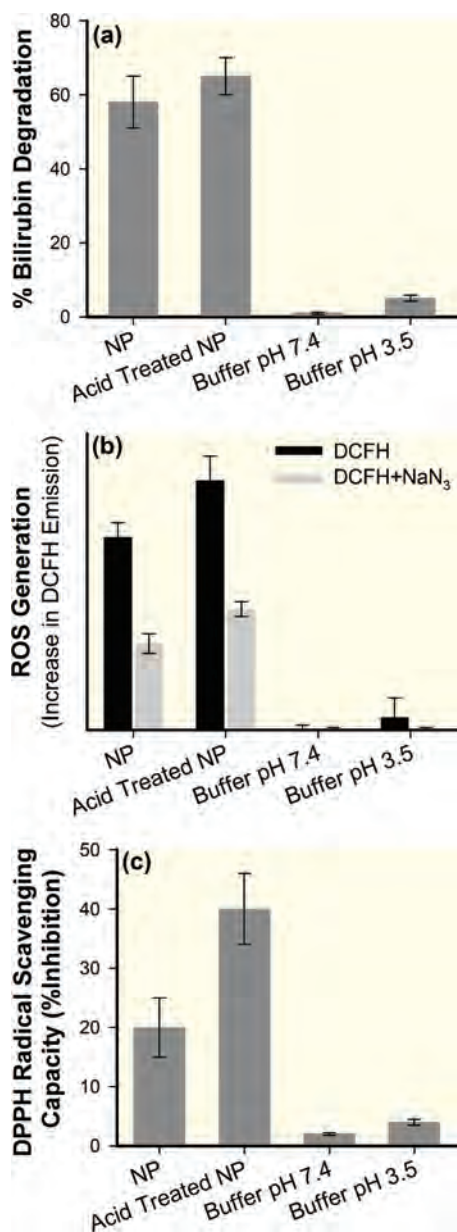


Fig. 2. Effect of acid treatment on activity of C-Mn₃O₄ NPs. (a) Bilirubin degradation after 45 mins. (b) ROS generation ability after 15 mins. (d) DPPH free radical scavenging activity after 1 hour.

into Mn^{2+} and Mn^{4+} which are highly reactive towards bilirubin.²⁵ In various studies, C-Mn₃O₄ NPs have shown a tendency to produce ROS in solution.²⁶ In this study emission intensity at 520 nm of nonfluorescent DCFH-DA was monitored with time to evaluate the extent of ROS generation. We observed an increase in ROS generation upon acid treatment (Fig. 2(b)). The nature of ROS was found to be singlet oxygen, as in presence of sodium azide, a well-known singlet oxygen quencher, emission of DCF reduced significantly (Fig. 2(b)). It is also well recognized that hepatoprotective effect of a compound greatly depends on its antioxidant capacity. So, we estimated the antioxidant activity of C-Mn₃O₄ NPs (both neutral and acid

treated) using DPPH method. Figure 2(c) clearly shows that C-Mn₃O₄ NPs hold substantial free radical scavenging activity which is significantly increased upon acid treatment. This antioxidant activity of C-Mn₃O₄ NPs may be due to the redox reaction between the Mn(II) and Mn(III) states due to LMCT. The formation of complex between Mn and an anion causes a decrease in the redox potential of the Mn(II) \leftrightarrow Mn(III) couple, enhancing the disproportionation of Mn(III) to Mn(II).^{27, 28}

In order to estimate the maximal-tolerated dose of C-Mn₃O₄ NPs, single-dose acute toxicity study was conducted following OECD guideline. No mortality was observed after oral administration of C-Mn₃O₄ NPs for all three dose groups. During the study period no behavioral and physical symptoms of acute toxicity such as decreased activity or decreased uptake of food and water were spotted.

The internalization of NPs from GI tract is very important for its therapeutic activity. So that, we estimated Mn content both in liver and circulation using ICP-AES. The results depict increased deposition of Mn in liver 12 hrs after treatment with C-Mn₃O₄ NPs (4.04 ± 0.2 g/gm tissue compared to 2.54 ± 0.1 g/gm tissue of Control; $p < 0.05$). The Mn content of blood also increased from 0.81 ± 0.1 g/ml to 1.54 ± 0.3 g/ml ($p < 0.05$) after 2 hrs of treatment.

CCl_4 is a well-known hepatotoxic agent extensively used to study hepatoprotective activity of new drugs in pre-clinical animal models of liver cirrhosis and fibrosis.²⁹⁻³¹ To evaluate the protective effect of C-Mn₃O₄ NPs against CCl_4 induced chronic hepatitis, structural changes in H/E stained liver sections were studied under microscope. Figure 3(a) illustrates the changes in outer morphology of the liver throughout experimental groups. Livers from group II and V have shown signs of CCl_4 toxicity. H/E stained liver sections of the vehicle control animals displayed a typical hepatic architecture with hepatic plates directed from the portal triads towards the central vein. In the CCl_4 -intoxicated mice (Group II, Fig. 3(b)), massive centrilobular necrosis, vacuolation, increased cellular mitosis and inflammatory infiltrations into the portal triads and distortion of CVs were detected. Liver sections from NPs (Group IV) and Silymarin (Group VI) treated groups showed better conservation of the normal liver architecture (Fig. 3(b)). All of these treated groups exhibited irregular periportal inflammatory infiltration, minor dilation of Disse space and restoration of compact liver structure. However, in comparison to NPs, conventional drug silymarin showed lesser activity as observed in hepatic morphological analysis. The animals treated with only C-Mn₃O₄ NPs (Group III, Fig. 3(b)) showed regular liver architecture similar to vehicle control group. Citrate displayed no or slight healing effect on hepatic morphology (Group V, Fig. 3(b)). To evaluate necroinflammatory changes, Ishak modified hepatic activity index and METAVIER system were used.^{32, 33} In the Ishak's and

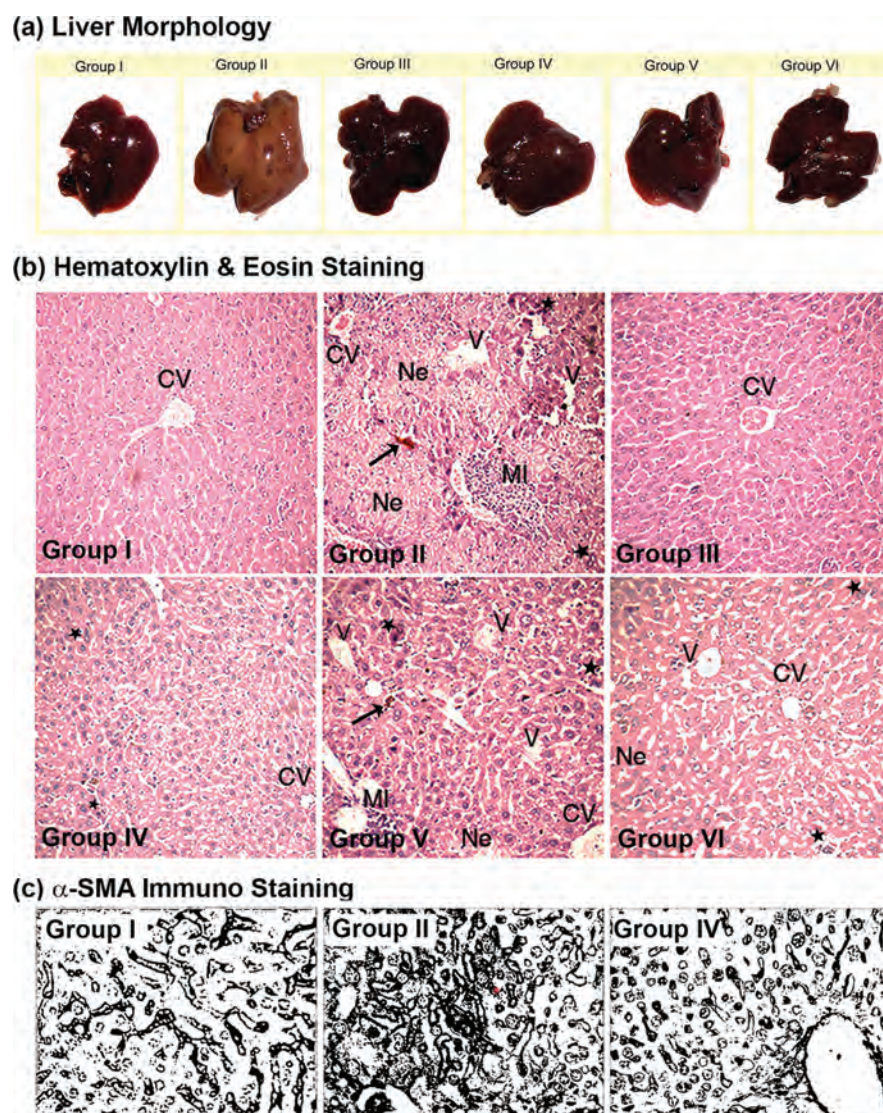


Fig. 3. Effect of C-Mn₃O₄ NPs on hepatic morphological analysis in CCl₄-intoxicated mice. (a) Representative photographs of liver after the experimental period. (b) Hematoxylin and eosin stained liver sections under microscope of Group I–VI. (c) α -SMA immunohistochemistry. Portal areas showed high immunoreactivity in case of CCl₄ treated mice. CV-central vein; Ne-necrosis, MI-mononuclear infiltration; *-increased mitotic activity; →-hemorrhage; V-vacuolation.

METAVIER grading, tissue sections from CCl₄ induced mice scored 14 (highest score possible is 18) and 3 (severe; highest score possible is 3) respectively. However, treatment with C-Mn₃O₄ NPs reduced it to level of the control (0 for both scoring). So, according to the microscopic examinations, severe cellular liver damage induced by CCl₄ was remarkably reduced by oral administration of the NPs.

CCl₄ is a well-known genotoxic agent that causes fibrosis of liver. Keeping that in mind we further performed immunostaining against α -SMA, a definitive marker of fibrotic liver. α -SMA immunoreactivity increases with increased ECM deposition. Figure 3(c) depicts liver sections stained with anti- α -SMA antibody (showing only α -SMA positive areas processed with Image J). In case of control animals, α -SMA immunopositivity was limited

to the smooth musculature belonging to the arterial tunica media, as well as to the wall of majority of portal and central veins, while other liver cells remain negative (Fig. 3(c), Control). CCl₄ strongly induced perisinusoidal α -SMA expression, which was recognized as activated HSCs, through affected lobule, connected between themselves with thin, “bridging” immunopositivity (Fig. 3(c), CCl₄). The livers of mice receiving C-Mn₃O₄ NPs displayed staining pattern alike control animal (Fig. 3(c), CCl₄ + NP) with infrequent α -SMA positivity. The calculated α -SMA positive area were shown in Figure 3(c). It is clear from the plot that CCl₄ treatment caused more than two fold increase in α -SMA level, which after treatment with NPs decreased to a level similar as control animals, representing an attenuation of the fibrogenic properties of HSCs. On the basis of histological outcomes, we

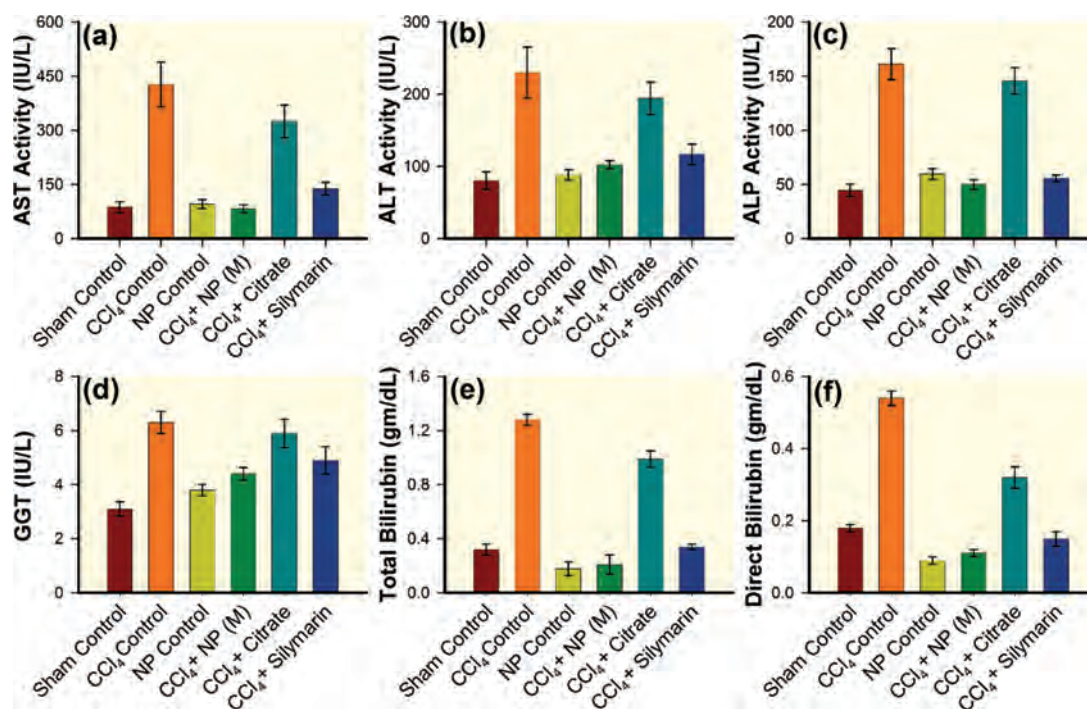


Fig. 4. Effect of C-Mn₃O₄ NPs on liver function enzyme activity in CCl₄-intoxicated mice. (a) AST (b) ALT (c) ALP (d) GGT (e) Total bilirubin (f) Direct Bilirubin.

applied scoring to the livers of different groups. Both Ishak and Ishak modified fibrosis staging was performed. After 6 weeks of CCl₄ administration, most mice had fibrous portal expansion with short fibrous septa (Ishak 3), and seldom proceeded to complete bridging fibrosis with appearance of a few of regenerative nodules (Ishak 4). However, treatment with C-Mn₃O₄ NPs reduced the degree of fibrosis, decreasing the score to normal.

Results of histopathological studies are further backed by alterations in serum biochemical parameters. The elevation in serum levels of AST and ALT (~400% and ~200% respectively) after CCl₄ treatment designates to the damaged structural integrity of the liver.³⁴⁻³⁶ Leakage of huge amounts of these enzymes from hepatocytes to the circulation is related to immense centrilobular necrosis, ballooning degeneration and cellular infiltration of the liver. Other hepatic biomarkers showed similar tendency. Elevated levels of ALP (~260%), GGT (~95%), TB (~350%), and DB (~210%) in serum further confirmed induction of chronic hepatitis by CCl₄. Two weeks treatment with C-Mn₃O₄ NPs at a dose of 1.5 ml (OD₄₃₀ 0.5)/kg BW decreased the elevated serum levels of aforementioned biomarkers to almost normal (AST ~ 90%, ALT ~ 60%, ALP ~ 75%, GGT ~ 35%, TB ~ 80%, DB ~ 70% compared to CCl₄ treated group; $p < 0.05$), inferring that C-Mn₃O₄ NPs tended to prevent damage and suppressed the leakage of enzymes. Treatment with silymarin also improved the liver parameters, but with lesser efficacy (AST ~ 60%, ALT ~ 50%, ALP ~ 60%,

GGT ~ 20%, TB ~ 70%, DB ~ 70% compared to CCl₄ treated group; $p < 0.05$). Moreover, it could not restore the above mentioned enzymes particularly AST and ALT (1.8 and 1.4 times higher respectively compared to control; $p < 0.05$) to normal level within the treatment period. This clearly indicates that, NPs could heal hepatic damage faster than the conventional drug Silymarin. The liver function parameters for the NP control group (group III) remained almost same as the vehicle treated group (group I). No significant improvement in the citrate control group confirmed that citrate alone is not playing any role in prevention of hepatotoxicity.

Our *in vitro* studies, as depicted in earlier section, have shown the antioxidant potential of C-Mn₃O₄ NPs. Therefore, to find its mechanism of action we targeted *in vivo* antioxidant defense system comprising of the trio; SOD, CAT and GPx.³⁷ SOD converts superoxide anions to H₂O₂, which is further converted to H₂O with the help of GPx and CAT. SOD also inhibits hydroxyl radical production.⁵ Sustaining the balance between ROS and antioxidant enzymes is critical for prevention of oxidative injury which can cause damage³⁸ to protein, lipids and DNA of a cell.⁵ Figure 5 shows that CCl₄ destructed the hepatic antioxidant enzymes causing significant decrease in hepatic SOD (~61%), CAT (~65%) and GPx (~60%) activities. Treatment with orally administered NPs and Silymarin substantially raised the antioxidant enzyme levels almost to normal. Citrate also exhibited some amount of efficacy in reversal of antioxidant defense mechanism.

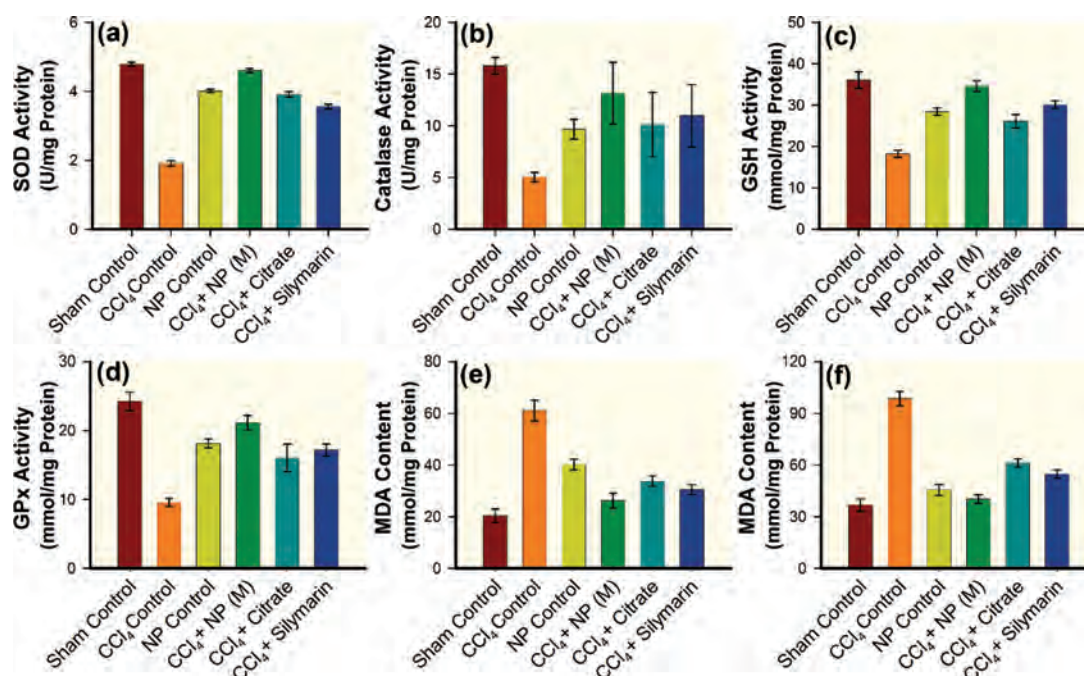


Fig. 5. Effects of orally treated C-Mn₃O₄ NPs on liver SOD, catalase, GPx, GSH and MDA content in CCl₄ intoxicated mice. (a) SOD activity (b) Catalase activity (c) GSH level (d) GPx activity (e) Serum MDA content (f) MDA content from liver homogenate.

In case of NP control group (Group III), some pro-oxidant effect was observed. This is because of the inherent property of the NPs to produce ROS in solution as described in our *in vitro* studies. However this change has not damaged the liver and it has no effect on liver marker enzymes. GSH, a non-enzymatic antioxidant, plays excellent role in protection of cells from CCl₄-induced hepatotoxicity.⁵ GSH combines with trichloromethyl radical, in presence of GST catalytic activity, which in turn contributes to detoxification of CCl₄. GSH stores are markedly exhausted, especially when liver necrosis initiates. In the current study, we noticed decline in hepatic GSH (~50%) level upon CCl₄ administration. Treatment with C-Mn₃O₄ NPs restored GSH level to the normal. The effect could either be due to the *de novo* synthesis of GSH, its regeneration, or both. Rapid membrane lipid peroxidation has been proposed as the basis of CCl₄ liver toxicity. So, we checked the levels of MDA, an index of oxidative damage and one of the decomposition products of peroxidised polyunsaturated fatty acids, to estimate the effect of C-Mn₃O₄ NPs' treatment on CCl₄-induced liver peroxidation. As shown in Figures 5(e and f), significant increase of MDA (~172% and ~205% respectively for hepatic and serum MDA content; $p < 0.05$) in the CCl₄-treated group confirmed that oxidative damage had been induced. Consistent with liver function tests, treatment with C-Mn₃O₄ NPs and Silymarin significantly reduced both hepatic (~55% and ~45% respectively; $p < 0.05$) and serum (~55% and ~50% respectively; $p < 0.05$) MDA content. The observed *in vivo* ability of C-Mn₃O₄ NPs in protection against lipid peroxidation and oxidative damage may involve various

mechanisms. Firstly, redox reaction between the Mn(II) and Mn(III) states in C-Mn₃O₄ NPs due to LMCT may help it to act as a scavenger of hydroxyl and superoxide radicals (details are discussed in previous section of the text). Secondly, it may act as a chain-breaker in inhibiting iron-induced lipid peroxidation chain reactions,^{39,40} and as proposed in other studies, Mn(II) may scavenge peroxy lipid radicals.^{41,42}

As mitochondria are a major site of ROS production, we further studied the effect of C-Mn₃O₄ NPs on it. Earlier studies portrayed the dependence of mitochondrial defense mechanisms on the cytosolic pool of reducing equivalents such as GSH. Depletion of these equivalents (also evident in our study) in the cytosol has direct consequences on the mitochondrial redox state. Previous studies revealed that COX plays a crucial role in oxidative stress and associated apoptosis.⁴³ In this study, the activity of COX found to be significantly decreased in CCl₄ treated mice (Fig. 6(a)), which is consistent with reported literature.⁴⁴⁻⁴⁶ Even though, treatment with C-Mn₃O₄ NPs has significantly ($p < 0.05$) improved COX activity, normal level was not restored. Ca²⁺-induced liver mitochondria permeability transition (MPT) is a useful model for evaluating the effects of drugs or other substances on mitochondrial function.⁴⁷ The mitochondria isolated from the CCl₄ intoxicated-group were more sensitive to Ca²⁺ as shown by a quick drop of 540 nm absorbance. C-Mn₃O₄ NPs attenuated Ca²⁺-induced MPT, as shown by slow decline of A₅₄₀ that mimicked the control group (Fig. 6(b)). This indicates a protective role of C-Mn₃O₄ NPs on normal MTP of mitochondria.

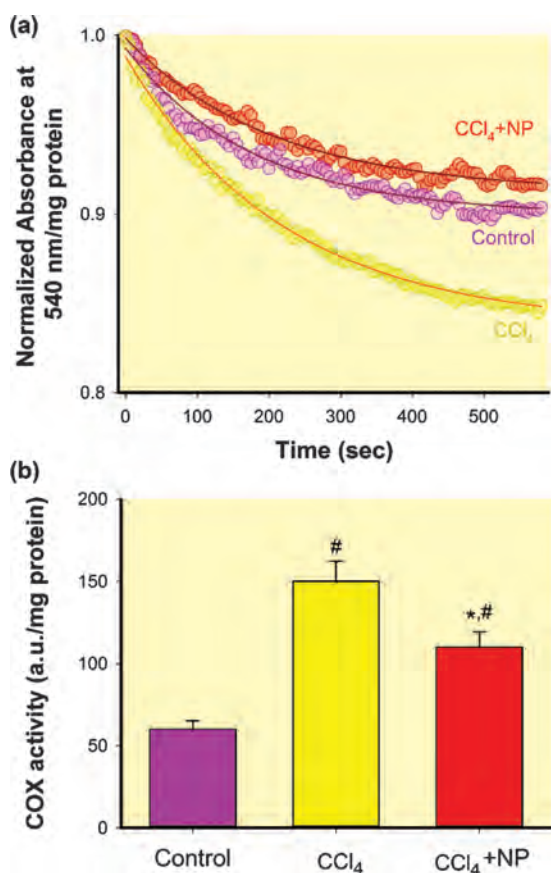


Fig. 6. Effect of C-Mn₃O₄ NPs on mitochondria. (a) Effect on mitochondria permeability transition (MPT), measured as decrease in absorbance at 540 nm. (b) Cytochrome c oxidase (COX) activity.

4. CONCLUSION

In conclusion, the present study showed, C-Mn₃O₄ NPs when administered orally can protect liver from CCl₄-induced chronic liver damages due to its increased antioxidant properties upon acid treatment in stomach. Its possible promising therapeutic role against oxidative stress and related chronic liver diseases deserves consideration. However, cautions must be taken as there is prevalent debate about nanotoxicity. Detailed toxicity study and more preclinical trials are required before it reaches the clinics for use in prevention of liver diseases.

Acknowledgment: Nabarun Polley thanks DST, India for Inspire Research Fellowship. Authors thank DAE (India) for financial grant, 2013/37P/73/BRNS. They also thank DST, India for financial grants, SB/S1/PC-011/2013. Authors thank SAIF, IIT Bombay for estimating the Mn content by ICP-AES.

References and Notes

1. T. A. Wynn and T. R. Ramalingam, *Nat Med.* 18, 1028 (2012).
2. D. C. Rockey, P. D. Bell, and J. A. Hill, *N. Engl. J. Med.* 372, 1138 (2015).

3. U. N. Statistics, <http://www.statistics.gov.uk/>, <http://www.statistics.gov.uk/>.
4. N. Polley, S. Saha, S. Singh, A. Adhikari, S. Das, B. R. Choudhury, and S. K. Pal, *J. Biomed. Opt.* 20, 067001 (2015).
5. H. Zhang, C.-H. Yu, Y.-P. Jiang, C. Peng, K. He, J.-Y. Tang, and H.-L. Xin, *PLoS ONE* 7, e46574 (2012).
6. P. Hall and J. Cash, *Ulster Med. J.* 81, 30 (2012).
7. M. Botros and K. A. Sikaris, *Clin. Biochem. Rev.* 34, 117 (2013).
8. R. Benyon and J. Iredale, *Gut.* 46, 443 (2000).
9. A. Eguchi, T. Yoshitomi, M. Lasic, C. D. Johnson, L. B. Vong, A. Wree, D. Povero, B. G. Papouchado, Y. Nagasaki, and A. E. Feldstein, *Nanomedicine.* 10, 2697 (2015).
10. S. Sha, L. B. Vong, P. Chonpathompikunlert, T. Yoshitomi, H. Matsui, and Y. Nagasaki, *Biomaterials* 34, 8393 (2013).
11. S. Lei, K. Tang, Z. Fang, and H. Zheng, *Cryst. Growth Des.* 6, 1757 (2006).
12. A. Giri, N. Goswami, M. Pal, M. T. Z. Myint, S. Al-Harathi, A. Singha, B. Ghosh, J. Dutta, and S. K. Pal, *J. Mater. Chem. C* 1, 1885 (2013).
13. S. Chaudhuri, S. Sardar, D. Bagchi, S. Dutta, S. Debnath, P. Saha, P. Lemmens, and S. K. Pal, *ChemPhysChem.* 17, 270 (2015).
14. M. Ohnishi, H. Morishita, H. Iwahashi, S. Toda, Y. Shirataki, M. Kimura, and R. Kido, *Phytochemistry* 36, 579 (1994).
15. OECD, *Test No. 423: Acute Oral Toxicity-Acute Toxic Class Method*, OECD Publishing (2001).
16. E. C. Jensen, *The Anatomical Record* 296, 378 (2013).
17. P. Manna, M. Sinha, and P. C. Sil, *BMC Complement Altern. Med.* 6, 33 (2006).
18. P. Kakkar, B. Das, and P. Viswanathan, *Indian J. Biochem. Biophys.* 21, 130 (1984).
19. C. Britton and A. Mehley, *Method in Enzymology* 2, 764 (1955).
20. G. L. Ellman, *Arch. Biochem. Biophys.* 82, 70 (1959).
21. J. M. Graham, *Biomembrane Protocols: I. Isolation and Analysis* 19, 29 (1993).
22. M. Spinazzi, A. Casarin, V. Pertegato, L. Salviati, and C. Angelini, *Nat. Protocols* 7, 1235 (2012).
23. N. Polley, S. Saha, A. Adhikari, S. Banerjee, S. Darbar, S. Das, and S. K. Pal, *Nanomedicine (Lond.)* 10, 2349 (2015).
24. A. Giri, N. Goswami, C. Sasmal, N. Polley, D. Majumdar, S. Sarkar, S. N. Bandyopadhyay, A. Singha, and S. K. Pal, *RSC Adv.* 4, 5075 (2014).
25. T. Takashima, K. Hashimoto, and R. Nakamura, *J. Am. Chem. Soc.* 134, 1519 (2012).
26. N. Polley, S. Saha, A. Adhikari, S. Banerjee, S. Darbar, S. Das, and S. K. Pal, *Nanomedicine* 10, 2349 (2015).
27. Y. Kozlov, A. Kazakova, and V. Klimov, *Membr. Cell Biol.* 11, 115 (1996).
28. M. J. Horsburgh, S. J. Wharton, M. Karavolos, and S. J. Foster, *Trends Microbiol.* 10, 496 (2002).
29. G. Tan, S. Pan, J. Li, X. Dong, K. Kang, M. Zhao, X. Jiang, J. R. Kanwar, H. Qiao, and H. Jiang, *PLoS One* 6, e25943 (2011).
30. L. W. Weber, M. Boll, and A. Stampfl, *Crit. Rev. Toxicol.* 33, 105 (2003).
31. L. Yuan and N. Kaplowitz, *J. Mam.* 30, 29 (2009).
32. E. M. Brunt, *Hepatology* 31, 241 (2000).
33. N. D. Theise, *Mod. Pathol.* 20, S3 (2007).
34. B. Huang, X. Ban, J. He, J. Tong, J. Tian, and Y. Wang, *Food Chem.* 120, 873 (2010).
35. R. O. Recknagel, E. A. Glende, J. A. Dolak, and R. L. Waller, *Pharmacol. Ther.* 43, 139 (1989).
36. G.-J. Huang, J.-S. Deng, S.-S. Huang, Y.-Y. Shao, C.-C. Chen, and Y.-H. Kuo, *Food Chem.* 132, 709 (2012).
37. M. Venukumar and M. Latha, *Indian J. Clin. Biochem.* 17, 80 (2002).
38. M. Taniguchi, T. Takeuchi, R. Nakatsuka, T. Watanabe, and K. Sato, *Life Sci.* 75, 1539 (2004).

39. I. Sziráki, K. P. Mohanakumar, P. Rauhala, H. G. Kim, K. J. Yeh, and C. C. Chiueh, *Neuroscience* 85, 1101 (1998).
40. I. Sziraki, P. Rauhala, K. K. Koh, P. van Bergen, and C. C. Chiueh, *Neurotoxicology* 20, 455 (1999).
41. K. Valachová, G. Kogan, P. Gemeiner, and L. Šoltés, *Interdiscip. Toxicol.* 3, 26 (2010).
42. M. Coassin, F. Ursini, and A. Bindoli, *Arch. Biochem. Biophys.* 299, 330 (1992).
43. S. Orrenius, V. Gogvadze, and B. Zhivotovsky, *Annu. Rev. Pharmacol. Toxicol.* 47, 143 (2007).
44. L. Knockaert, A. Berson, C. Ribault, P.-E. Prost, A. Fautrel, J. Pajaud, S. Lepage, C. Lucas-Clerc, J.-M. Bégué, and B. Fromenty, *Lab. Invest.* 92, 396 (2012).
45. C. Mitchell, M.-A. Robin, A. Mayeuf, M. Mahrouf-Yorgov, A. Mansouri, M. Hamard, D. Couton, B. Fromenty, and H. Gilgenkrantz, *Am. J. Pathol.* 175, 1929 (2009).
46. A. Adhikari, N. Polley, S. Darbar, D. Bagchi, and S. K. Pal, *Future Science OA* 2, FSO146 (2016).
47. J. Gao, X. Tang, H. Dou, Y. Fan, X. Zhao, and Q. Xu, *J. Pharm. Pharmacol.* 56, 1449 (2004).